THE JOURNAL OF PHYSICAL CHEMISTRY B

Article

pubs.acs.org/JPCB

Investigation of Optical Nonlinearities and Transient Dynamics in a Stilbenzene Derivative

Junyi Yang,[†] Yinglin Song,*[,†,§] Weiju Zhu,[‡] Xinyan Su,[‡] and Hongyao Xu*[,‡]

[†]School of Physical Science and Technology, Soochow University, Suzhou 215006, P. R. China

[‡]College of Material Science and Engineering & State Key Laboratory for Modification of Chemical Fibers and Polymer Materials, Donghua University, Shanghai 201620, China

[§]Department of Physics, Harbin Institute of Technology, Harbin 150001, P. R. China

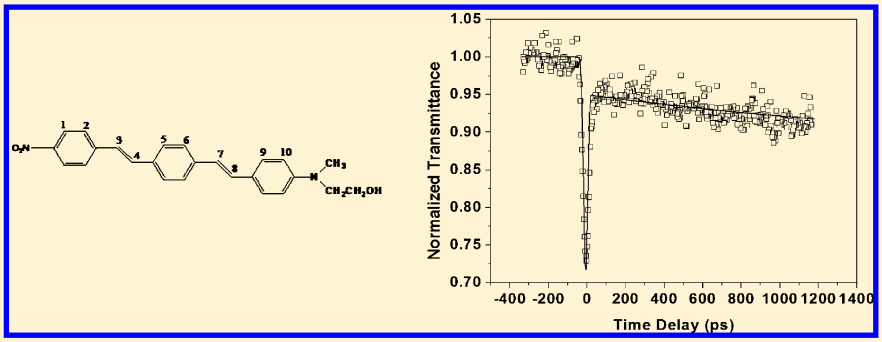

ABSTRACT: The temporal properties of nonlinear absorption of a stilbenzene derivative have been investigated by time-resolved pump−probe techniques with picosecond laser pulses at the wavelength of 532 nm. With the help of an additional nanosecond and picosecond open-aperture Z-scan technique, numerical simulations based on a new five-energy level model are used to interpret the experimental results, and the nonlinear optical parameters of this new compound are determined. The five-energy level model is described by two-photon absorption (TPA) excited from ground-state-induced excited-state absorption (ESA) including singlet ESA and triplet ESA. Under the nanosecond pulse excitation, a TPA excited from the triplet excited state contributes to the nonlinear absorption, and the value of the TPA is found to be 1 order of magnitude larger than those usually found for TPA excited from the ground state.

INTRODUCTION

Recently, various new compounds with large two-photon absorption (TPA) cross sections have been investigated extensively for their potential applications in optical data storage,[1] photodynamic therapies,[2] up-conversion lasing,[3] three-dimensional (3D) microfabrication,[4] two-photon fluorescence imaging,[5] and optical limiting.[6] Compared with inorganic materials, conjugated organic materials are more predominant in properties such as large third-order nonlinear optical susceptibility, fast response, high resistance to laser radiations, low dielectric constant, and ease of processing, so organic materials design, synthesis, and structure−property research have been issues for materials investigation. In order to design effective organic compounds for third-order NLO applications, researchers have obtained much valuable experience for large TPA cross section molecular design strategies, including donor−acceptor−donor (D−A−D),[7,8] donor−π−donor (D−π−D),[9,10] donor−π−acceptor (D−π−A), and acceptor−π−acceptor (A−π−A)[11,12] types of molecules. One good method is to end-cap a suitable conjugated bridge with donor and acceptor substituent. So far, many organic D−π−A compounds have been studied experimentally and theoretically, including derivatives of benzene, azobenzene, styrene, and stilbene.[13−23] Among these organic D−π−A compounds, stilbene derivatives have attracted much attention due to potential applications in fields of pharmaceutical chemistry.[24] The studies indicate that organic D−π−A compounds are highly promising candidates for NLO applications. Theoretically, a three-level model of TPA-induced excited-state absorption (ESA) is always used to explain nonlinear absorption of these organic compounds.[25]

In this paper, the syntheses and nonlinear absorption of a long conjugated stilbenzene derivative 2-(methyl(4-((*E*)-4-((*E*)-4-nitrostyryl)styryl)phenyl)amino)ethanol is reported. The nonlinear absorption of this compound in *N*,*N*′-dimethylformamide (DMF) was investigated by using Z-scan technique[26] with nanosecond and picosecond pulses. The nonlinear optical mechanism of the solution is studied by the picosecond time-resolved pump−probe measurement. A new rate rate-equation model is established to explain nonlinear absorption of this compound. Comparing the results of pump−probe and Z-scan measurements to the rate-equation model, the values for the excited-state lifetime, the excited-state

Received: August 16, 2011
Revised: December 16, 2011
Published: January 6, 2012

absorption cross section, and the cross section of TPA are obtained.

SAMPLE PREPARATION AND EXPERIMENT

Synthesis of 2-(Methyl(4-((*E*)-4-((*E*)-4-nitrostyryl)-styryl)phenyl)amino)ethanol (A3). The compound **A3**, as shown in Figure 1, was prepared through a multistep synthesis

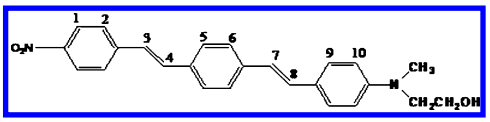

Figure 1. Molecular structure of the new compound **A3**.

route. First, 2-((4-formylphenyl)(methyl)amino)ethyl acetate was obtained from 2-(methyl(phenyl)amino)ethanol by esterification and oxidation reaction. Then, treatment of 2-((4-formylphenyl)(methyl)amino)ethyl acetate with 1-bromo-4-(bromomethyl)benzene, followed by a Heck reaction with 1-nitro-4-vinylbenzene, yielded the objective compound with an asymmetrical D−π−A structure. The detailed synthesis process will be described in other articles. Yield: 67%. FT-IR (KBr, cm^{-1}): 3392 (OH), 2918, 2851 (CH_3), 1338 (NO_2), 962 (trans =C−H, out-of-plane bending vibration). ^{1}H NMR (DMSO, 400 MHz, ppm), δ 2.97 (s, 3H, CH_3), 3.43 (t, 2H, J = 5.2 Hz, NCH_2CH_2OH), 3.56 (t, 2H, J = 5.2 Hz, NCH_2CH_2OH), 4.68 (s, H, O*H*), 6.71 (d, 2H, J = 8.8 Hz, H^1), 6.97 (d, 1H, J = 16.4 Hz, H^7), 7.20 (d, 1H, H^8), 7.42 (d, 2H, J = 15.6 Hz, $H^{3,4}$), 7.58 (m, 6H, J = 7.6 Hz, $H^{2,5,6}$), 7.86 (d, 2H, J = 8.8 Hz, H^9), 8.24 (d, 2H, H^{10}). Both IR and ^{1}H NMR signals provide unequivocal proof of the structure of the *trans*−*trans* isomer, and the purity of the isomer was constantly monitored by HPLC to be greater than 97% during the experimental

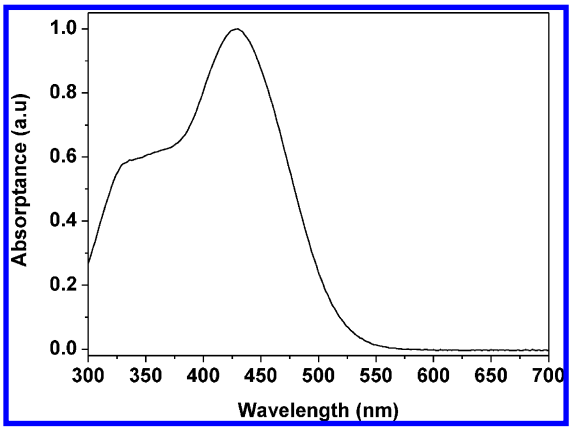

Figure 2. Normalized absorption spectra of the compound at a concentration of 1 × 10^{-5} M.

conditions. Figure 2 shows the UV−vis spectra of compound **A3**.

Nonlinear Optical Measurements. The nonlinear optical absorption of the **A3** solution is measured by the Z-scan technique using a Nd:YAG 532 nm laser (Continuum, Surelite II) with a pulse width 4 ns (fwhm) and a mode-locking Nd:YAG 532 nm laser (EKSPLA, PL2143B) with a pulse width 21 ps (fwhm), repetition rate of 2 Hz, respectively. The spatial distribution of the pulse is nearly a Gaussian profile. The sample solution was placed in quartz cells of 2 mm thickness. The quartz cell with the sample was placed on a translation stage controlled by a computer that moved the sample along the z-axis with respect to the focal point of a 400 mm focal lens. The laser pulses adjusted by an attenuator are separated into two beams by using a splitter. The two beams were simultaneously measured by using two energy detectors (Rjp-765 energy probe) linked to an energy meter (Rj-7620 ENERGY RATIOMETER, Laserprobe). A personal computer is used to collect data coming from energy meter through a GPIB interface. The measurement system was calibrated with CS_2.

In the pump−probe experiments, the same laser source as the one used in the picosecond Z-scan measurement is used. The pump−probe experimental setup was a standard one, and the probe peak irradiance was approximately 8% of the pump irradiance.[27] The sample cell thickness is 2 mm. The focal length of the lens is f = 400 mm. The probe waist (29 μm) is smaller than the pump waist (50 μm). A variable delay is introduced into the probe path, and the two pulses are recombined at the sample cell at a small angle (4°). The energy of the pump beam is 6.6 μJ. The probe peak irradiance was approximately 8% of the pump peak irradiance. The small angle between the beams and the fact that the probe spot size is considerably smaller than the pump ensure that the probe could test a uniformly excited region of material in the 2 mm cell, and the effective acting thickness is about 0.77 mm according to a calibration. The polarization of the pump beam was rotated by 90° with respect to that of the probe beam with polarizer to avoid interference. The change of the probe beam intensity versus the delay time is recorded after the pump beam. The laser pulses adjusted by an attenuator are separated into two beams by using a splitter.

RESULTS AND DISCUSSION

Optical Properties of A3. As shown in Figure 2, strong absorption peaks are located at 430 nm, which are assigned to π−π^* electronic transitions of the conjugated molecules. Compound **A3** is soluble in common organic solvents such as DMF, and the concentration of compound **A3** used in our experiment is 7.4 × 10^{-4} mol/L in DMF, corresponding to a number density of 4.43 × 10^{23} m^{-3}.

Figure 3 gives the nonlinear absorption properties of the **A3** solution with 4 ns and 21 ps pulse under an open-aperture Z-scan configuration. It shows that the compound **A3** has strong nonlinear absorption under the 4 ns pulse and the 21 ps pulse excitation. Because the solvent DMF shows no nonlinear absorption under the identical experimental conditions, the observed nonlinear absorption effect should originate from the solute **A3**. The valley of the normalized transmittance indicates that the laser pulses experience strong reverse saturable absorption (RSA). Moreover, to gain an insight into the nonlinear origin of the compound solution, the picosecond time-resolved pump−probe experiments have been performed at 532 nm on the solution. The experimental result is shown in Figure 4. The pump−probe signal of the solution consists of three components: an ultrafast valley near the zero point and fast recovery and slow decay components, which indicate that the mechanism of the nonlinear absorption may be explained by the TPA-induced ESA model.[12,25] However, it must be noted that the linear absorption cannot be neglected at 532 nm, so the TPA-induced excited-state model may be unsuitable for explaining our experimental results. We have tried to use this model and several models to fit our experimental results,

dx.doi.org/10.1021/jp2078665 | J. Phys. Chem. B 2012, 116, 1221−1225

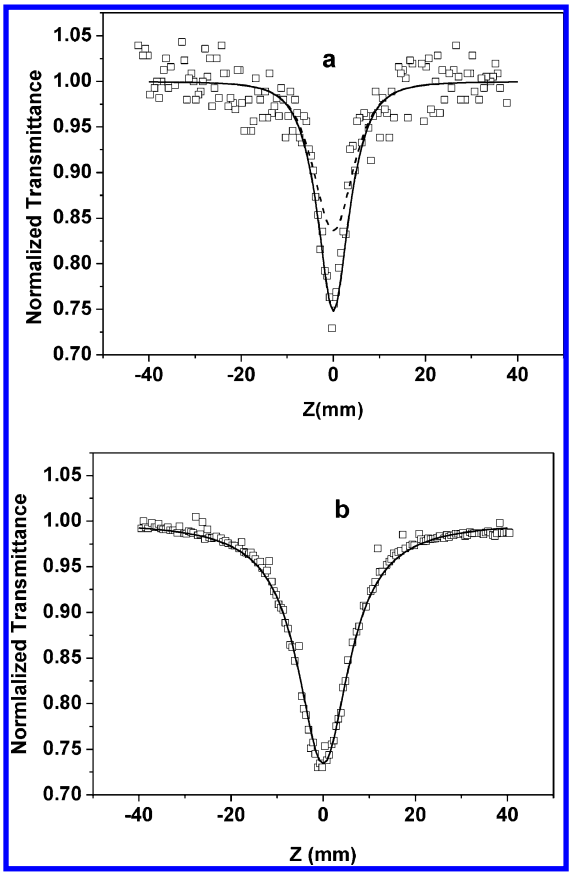

Figure 3. (a) Open aperture Z-scans curve of **A3** solution for 4 ns pulse width. (b) Open aperture Z-scans curve of **A3** solution for 21 ps pulse width. The squares represent experimental data; the dashed line and solid lines are theoretical fitting curves.

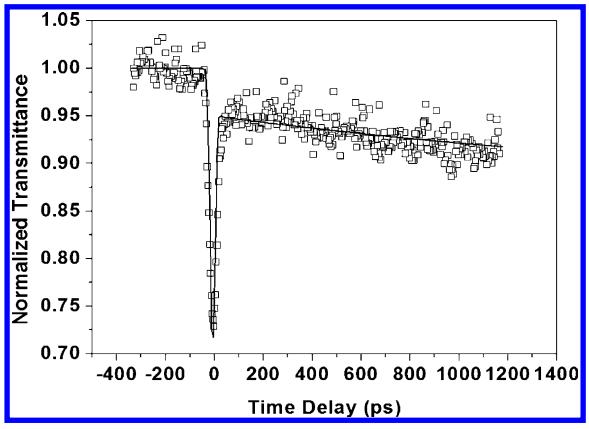

Figure 4. Pump−probe result for **A3**. The squares represent experimental data, and the solid line is the theoretical fitting curve.

including the 4 ns, 21 ps Z-scan and the pump−probe results; however, there are some poor simulations for the Z-scan or pump−probe experimental results simultaneously, except a five-level model, in which there is a triplet excited-state-induced TPA.

Model Interpretation. The new five-level model used to describe the optical nonlinear mechanism of the compound **A3** is shown in Figure 5. The process of absorption in the five-level system can be described briefly as follows. It is assumed that linear absorption promotes electrons from the ground state S_0 to the first excited singlet state S_1. Meanwhile, via two-photon

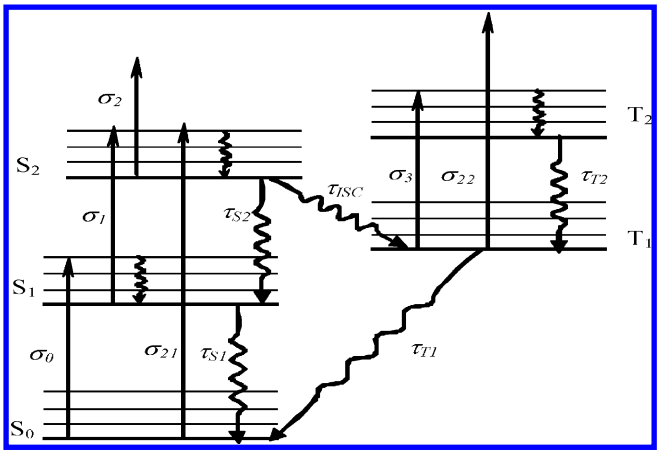

Figure 5. Five-level model for the nonlinear absorption behavior of **A3**. S, singlet states; T, triplet states.

excitations, $S_0 \rightarrow S_2$, the electrons are promoted from the ground state S_0 to the high excited singlet state, S_2, from which three processes can occur: the electron can relax back to S_1 by nonradiative transition $S_2 \rightarrow S_1$; the other is absorbing another photon and promoting the electron to a higher excited singlet state, S_3 (i.e., one-photon excitations $S_2 \rightarrow S_3$), from which it rapidly relaxes to S_2 with nonradiative transition $S_3 \rightarrow S_2$; however, the lifetime of S_3 is very short, and this state can be neglected under our experimental conditions; the third possibility is for the electron to undergo a spin-flip transition to the lowest triplet state T_1, and this process is called intersystem crossing. From the state S_1, two things may happen. The electron can relax to the ground state S_0 by a radiative or nonradiative transition. Another possibility is that the molecule may absorb another photon, which promotes the electron to a high excited singlet state S_2. For an electron in the lowest triplet state T_1, three possibilities exist. It may relax by phosphorescence to the ground state S_0. The other possibility is that the molecule absorbs another photon, promoting the electron to a higher-lying triplet state T_2. The electron then relaxes very rapidly back to the lowest triplet state T_1. The third process is that the electrons are promoted from the state T_1 to the higher excited singlet state T_3, by two-photon excitations, $T_1 \rightarrow T_3$, and the lifetime of the state T_3 is very short and then can be neglected.

These processes can be described easily by the rate equations

$$\frac{dN_0}{dt} = -\frac{\sigma_0 I_e N_0}{\hbar\omega} + \frac{N_1}{\tau_{s1}} + \frac{N_3}{\tau_{T1}} - \frac{\sigma_{21} I_e^2 N_0}{2\hbar\omega} \quad (1)$$

$$\frac{dN_1}{dt} = -\frac{\sigma_1 I_e N_1}{\hbar\omega} + \frac{\sigma_0 N_0 I_e}{\hbar\omega} - \frac{N_1}{\tau_{s1}} + \frac{N_2}{\tau_{S2}} \quad (2)$$

$$\frac{dN_2}{dt} = \frac{\sigma_1 I_e N_1}{\hbar\omega} - \frac{N_2}{\tau_{S2}} - \frac{N_2}{\tau_{ISC}} + \frac{\sigma_{21} I_e^2 N_0}{2\hbar\omega} \quad (3)$$

$$\frac{dN_3}{dt} = -\frac{\sigma_2 I_e N_3}{\hbar\omega} + \frac{N_1}{\tau_{ISC}} - \frac{N_3}{\tau_{T1}} + \frac{N_4}{\tau_{T2}} - \frac{\sigma_{22} I_e^2 N_3}{2\hbar\omega} \quad (4)$$

dx.doi.org/10.1021/jp2078665 | J. Phys. Chem. B 2012, 116, 1221−1225

$$\frac{dN_4}{dt} = \frac{\sigma_2 I_e N_3}{\hbar\omega} - \frac{N_4}{\tau_{T2}} + \frac{\sigma_{22} {I_e}^2 N_3}{2\hbar\omega} \quad (5)$$

and the intensity transmitted through sample is

$$\frac{dI_e}{dz'} = -(\sigma_0 N_0 + \sigma_1 N_1 + \sigma_2 N_3 + \sigma_{21} N_0 I_e + \sigma_{22} N_3 I_e) I_e \quad (6)$$

$$\frac{dI_p}{dz'} = -(\sigma_0 N_0 + \sigma_1 N_1 + \sigma_2 N_3 + \sigma_{21} N_0 I_e + \sigma_{22} N_3 I_e) I_p \quad (7)$$

with

$$I_e(z=0) = I_{oe} \frac{{\omega_{oe}}^2}{{\omega_e}^2} \exp\left[-\frac{2r^2}{{\omega_e}^2} - \frac{(t-t_d)^2}{\tau^2} \right] \quad (8)$$

$$I_p(z=0) = I_{op} \frac{{\omega_{op}}^2}{{\omega_p}^2} \exp\left(-\frac{2r^2}{{\omega_e}^2} - \frac{t^2}{\tau^2} \right) \quad (9)$$

where I_e and I_p are the irradiance of the pump beam and probe beam, respectively. $\omega_i(z) = \omega_{0i}[1 + (z/z_{0i})^2]^{1/2}$ (i = p, e) is the probe-beam and pump-beam radius at z, respectively. z is the sample position away from the focus on the axis, $z_{0i} = \pi {\omega_{0i}}^2/\lambda$ is the diffraction length of the beam, ω_{0i} (i = e, p) is the beam radius at focus, I_{0i} is the on-axis peak irradiance at focus and can be calculated from $I_{0i} = 2E_i/(\pi^{3/2}{\omega_{0i}}^2\tau)$, E_i(i = p, e) is the pulse energy, and τ is the laser pulse width (HW $1/e$). t_d is the time delay between the pump and probe. σ_0 is the ground-state absorption cross section, σ_1, σ_2, and σ_3 are the excited-state absorption cross sections from states S_1, S_2, and T_1, respectively; σ_{21} and σ_{22} are the TPA cross sections of states S_0 and T_1; N_0, N_1, N_2, N_3, and N_4 represent the number densities of states S_0, S_1, S_2, T_1, and T_2, respectively; z' is the propagation length in sample. τ_{ISC} is the intersystem crossing time; τ_{S1}, τ_{T1}, and τ_{T2} are the relaxation times of the first excited singlet state, the first excited triplet state, and the high excited triplet state, respectively.

As shown in Figure 4, the normalized transmittance consists of a valley near zero time delay and a slow-decaying tail at longer delays. The valley is due to TPA from the ground state S_0. The slow decaying tail is almost attributed to the higher singlet-state S_2 absorption and the triplet-state T_1 absorption induced by TPA and the singlet-state absorption. It is very interesting that with the delay time longer, the value of the tail is lower. These belong to the long lifetime of excited triplet state T_1 which also has larger cross sections than the one of higher singlet excited-state S_2 and ground-state S_0. The valley bottom of the transmission near zero delay is primarily sensitive to the TPA cross section of states S_0, σ_{21}. The degree of the recovery transmittance is mostly determined by the higher excited singlet state cross section σ_2 and the intersystem crossing time τ_{ISC}. Here, the absorption cross section of the first singlet excited state which for existence of the linear absorption is equal to σ_0. The long low tail of the curve is determined by two key parameters: the absorption cross section of excited triplet state σ_3 and the intersystem crossing time τ_{ISC}. In our model, the singlet excited-state supports the populations to the triplet state T_1; moreover, we estimate $\tau_{ISC} \geq 3$ ns according to the slow increase of the absorption which induces the long transmittance tail after the zero delay time as shown in Figure 4. So the relaxation time of the singlet state S_2 must to be several nanoseconds, and we estimate it to be $\geq$10 ns. The lifetime of the triplet state T_2 is considerably shorter than the pulse duration and can be neglected. The lifetimes of the S_1 and T_1 are very long and are estimated to be several microseconds. Here, $\sigma_0 = 6.41 \times 10^{-18}$ cm^2, which is provided by the linear absorption measurements, and the linear transmittance measurement is 54%. The two parameters σ_2 and σ_3 can be determined according to the long transmittance tail when we fit the theoretical curve to the experimental results. For these conditions, to solve the rate equations and fit the data allows us to uniquely extract σ_2 and σ_3.The theoretical curve superposed on the data in Figure 4 is obtained using a single set of parameters, $\sigma_1 = 6.41 \times 10^{-18}$ cm^2, $\sigma_2 = 8.59 \times 10^{-18}$ cm^2, $\sigma_3 = 1.03 \times 10^{-17}$ cm^2, and the cross section of TPA $\sigma_{21} = 9 \times 10^{-18}$ cm^4/GW. Here, $I_{0e} = 2.4 \times 10^{14}$ W/m^2. It is confirmed that the theoretical fitting is in good agreement with the experimental result. The higher singlet state S_2 has a larger absorption cross section than the ground state S_0 and the TPA from the ground state, which results in RSA as shown in Figure 3b under the 21 ps laser pulse excitation. The parameters used in theoretical fitting are those obtained according to the pump−probe experiment as discussed above. In the picosecond case, ω_0 is about 29 μm, and I_0 is 2.32×10^{13} W/m^2.

The long lifetime and the large absorption of the first triplet state T_1 result in the long low transmittance tail. However, we find that the parameters obtained above cannot fit the nanosecond Z-scan experimental data well. The theoretical fitting curve is shown in Figure 3a with the dashed line. Obviously, the valley of the experimental result is larger than that of the theoretical fitting. It is indicated that there is another absorption mechanism contributing to the nanosecond nonlinear absorption. However, this mechanism must have little influence on the pump−probe experimental results. So we think that there is a TPA process in the triplet excited state T_1. Once the pump pulse has passed through the sample, after the zero delay time, the TPA has little effect on the long transmittance because the intensity of pump beam is very small. The TPA cross section σ_{21} can be ascertained only by the nanosecond Z-scan experiment. A good theoretical fitting line is shown in Figure 3a and is obtained using the parameter $\sigma_{22} = 1.3 \times 10^{-16}$ cm^4/GW. The value of σ_{21} shows that a very large nonlinear response is found for this process which starts from an excited state. The value of σ_{22} is, in fact, orders of magnitude larger than those observed for molecules excited from their ground state. The first triplet excited state T_1 has a larger absorption cross section than the ground state S_0, which results in RSA. In the nanosecond case, ω_0 is about 23 μm, I_0 is 3.7×10^{12} W/m^2. The excellent agreement between the numerical simulations and the data reported here indicates that this new five-level model can accurately describe the photophysical dynamics of the sample.

The above discussions indicate that the results of the pump−probe experiment are consistent with the results of the Z-scan measurement. We can make a confirmation that the dominant nonlinear absorption mechanism of the **A3** solution is TPA combined with excited-state absorption. The nanosecond nonlinear absorption can be attributed mostly to triplet−triplet state absorption and the TPA excited from the state T_1, while the picosecond absorption data is attributable to the singlet

dx.doi.org/10.1021/jp2078665 | J. Phys. Chem. B 2012, 116, 1221−1225

excited-state absorption and TPA excited from the ground state S_0.

CONCLUSION

In summary, we have investigated the optical nonlinear absorption of compound **A3** in DMF solution by using the time-resolved pump−probe and the open Z-scan technique with 4 ns and 21 ps laser pulses at 532 nm. The experimental result of time-resolved pump−probe showed that the mechanism of nonlinear absorption for the compound **A3** includes ESA and TPA. Under the nanosecond pulses excitation, nonlinear absorption is dominantly induced by the singlet excited-state absorption and TPA excited from the ground state. On the other hand, the nanosecond nonlinear absorption can be attributed mostly to triplet−triplet state absorption and the TPA excited from the state T_1. The key photophysical parameters of **A3** were obtained by the pump−probe and Z-scan measurements.

AUTHOR INFORMATION

Corresponding Author

*E-mail address: ylsong@suda.edu.cn (Y.S.), hongyaoxu@163.com (H.X.).

ACKNOWLEDGMENTS

We gratefully acknowledge the National Natural Science Fund of China (Grant No. 90922007) and A Project Funded by the Priority Academic Program Development of Jiangsu Higher Education Institutions (PAPD).

REFERENCES

(1) Corredor, C. C.; Huang, Z. L.; Belfield, K. D. *Adv. Mater.* **2006**, *8*, 2910.
(2) Frederiksen, P. K.; Jørgensen, M.; Ogilby, P. R. *J. Am. Chem. Soc.* **2001**, *123*, 1215.
(3) He, G. S.; Yuan, L. X.; Cui, Y. P.; Li, M.; Prasad, P. N. *J. Appl. Phys.* **1997**, *81*, 2529.
(4) Sun, H. B.; Matsuo, S.; Misawa, H. *Appl. Phys. Lett.* **1999**, *74*, 786.
(5) Hell, S. W.; Hänninen, P. E.; Kuusisto, A.; Schrader, M.; Soini, E. *Opt. Commun.* **1995**, *117*, 20.
(6) Ehrlich, J. E.; Wu, X. L.; Lee, I.-Y.; Hu, S. Z.-Y.; Röckel, H.; arder, S. R.; Perry, J. W. *Opt. Lett.* **1997**, *22*, 1843.
(7) Susumu, K.; Fisher, J.A. N.; Zheng, J.; Beratan, D. N.; Yodh, A. G.; Therien, M. J. *J. Phys. Chem. A* **2011**, *115*, 5525.
(8) Gadisa, A.; Mammo, W.; Andersson, L. M.; Admassie, S.; Zhang, F.; Andersson, M.□R.; Inganäs, O. *Adv. Funct. Mater.* **2007**, *17*, 3836.
(9) Albota, M.; Beljonne, D.; Brédas, J.; Ehrlich, J. E.; Fu, J. Y.; Heikal, A. A.; Hess, S. E.; Kogej, T.; Levin, M. D.; Marder, S. R.; Dianne, M. M.; Perry, J. W.; Röckel, H.; Rumi, M.; Subramaniam, G.; Webb, W. W.; Wu, X. L.; Xu, C. *Science* **1998**, *281*, 1653.
(10) Li, Q. Q.; Huang, J.; Zhong, A. S.; Zhong, C.; Peng, M.; Liu, J.; Pei, Z. G.; Huang, Z. L.; Qin, J. G.; Li, Z. *J. Phys. Chem. B* **2011**, *115*, 4279.
(11) Cao, D. X.; Liu, Z. Q.; Fang, Q.; Xu, G. B.; Xue, G.; Liu, G. Q.; Yu, W. T. *J. Organomet. Chem.* **2004**, *689*, 2201.
(12) Li, C. W.; Yang, K.; Feng, Y.; Su, X. Y.; Yang, J. Y.; Jin, X.; Shui, M.; Wang, Y. X.; Zhang, X. R.; Song, Y. L.; Xu, H. Y. *J. Phys. Chem. B* **2009**, *113*, 15730.
(13) Abdel-Halim, H. M. *J. Chem. Phys.* **2003**, *119*, 484.
(14) Beck, B.; Grunmt, U. W. *J. Phys. Chem. B* **1998**, *102*, 664.
(15) Karamanis, P.; Maroulis, G. *Chem. Phys. Lett.* **2003**, *376*, 403.
(16) Cheng, L. T.; Tam, W.; Mrder, S. R.; Stiegman, A. E.; Rikken, G.; Spangler, C. W. *J. Am. Chem. Soc.* **1991**, *95*, 10643.
(17) Mandal, K.; Kar, T.; Nandi, F. *Chem. Phys. Lett.* **2003**, *376*, 116.
(18) Lambert, C.; Stadler, S.; Bourhill, C.; Brauchle, C. *Angew. Chem., Int. Ed. Engl.* **1996**, *35*, 644.
(19) Bartkowiak, W.; Zalesny, R.; Leszczynski, J. *Chem. Phys.* **2003**, *287*, 103.
(20) Marder, S. R.; Beratan, D. N.; Cheng, L. T. *Science* **1991**, *252*, 103.
(21) Yang, M. L.; Jiang, Y. S. *Phys. Chem. Chem. Phys.* **2001**, *3*, 167.
(22) Machado, A. E. D.; da Gama, A. A. S. *J. Mol. Struct. Theochem.* **2003**, *620*, 21.
(23) Dulcic, A.; Flytzanis, C.; Tang, C. L.; Pepin, D.; Fetizon, M.; Hoppilliard, Y. *J. Chem. Phys.* **1981**, *74*, 1559.
(24) Mahyar-Roemer, M.; Karsen, A.; Mestres, P.; Roemer, K. *Int. J. Cancer* **2001**, *94*, 615.
(25) Gu, B.; Ji, W.; Huang, X. Q.; Patil, P. S.; Dharmaprakash, S. M. *Opt. Express* **2009**, *17*, 1126.
(26) Sheik-Bahae, M.; Said, A. A.; Wei, T. H.; Hagan, D. J.; VanStryland, E. W. *IEEE J. Quantum Electron.* **1990**, *26*, 760.
(27) Xia, T.; Dogariu, A.; Mansour, K.; Hagan, D. J.; Said, A. A.; Van Stryland, E. W.; Shi, S. *J. Opt. Soc. Am. B.* **1998**, *15*, 1497.